

Fractional-order PID controller tuning using continuous state transition algorithm

Fengxue Zhang¹ · Chunhua Yang¹ · Xiaojun Zhou¹ · Weihua Gui¹

Received: 28 June 2016 / Accepted: 6 September 2016
© The Natural Computing Applications Forum 2016

Abstract Theoretical and applied studies of fractional-order $PI^{\lambda}D^{\mu}$ (FOPID) controller in many scientific and engineering fields have shown many advantages compared to the classical PID control. However, the adjustment of FOPID controller becomes more complicated due to two additional parameters. In this study, the FOPID controller adjustment problem is transformed into a nonconvex optimization problem, and then a new metaheuristic method, named state transition algorithm (STA), is introduced to select the optimal FOPID controller parameters. In the meanwhile, the influence of objective criterion and sample size on the performance of FOPID controller design is analyzed. The dominance of the proposed method, especially for tuning FOPID controller parameters, is attested by several simulation cases and the comparisons of STA with other stochastic global optimization algorithms over the same problems.

Keywords Fractional-order control · $PI^{\lambda}D^{\mu}$ · State transition algorithm · Objective criterion · Sample size

1 Introduction

Proportional-integral-derivative (PID) controller has been applied to real-world industrial process control for several decades. It is perhaps the most widely used controller in practical applications. The designing simplicity and performance superiority with low percentage

overshoot and short settling time in slow process plants contribute to its popularity [1]. In recent years, several research communities pay great attention to fractional-order controller and system, which are on the basis of fractional-order calculus [2, 3], due to the fact that numerous practical control systems can be expressed by fractional-order differential equations [4]. The most important goal of the use of fractional calculus is the application of the fractional-order controller (FOC) for the enhancement of the performance of system control. For instance, Podlubny [5] put forward the structure of the FOPID controller and illustrated the availability of such controller for actuating the response of fractional-order system. In [6], the authors proposed a new controller of fractional-order fuzzy proportional-integral-derivative (PID), which can be used on the closed-loop error reduction, and its fractional derivative and integrator are regarded as the input and the output, respectively. Koksai presented the application of a fractional-order $PI^{\lambda}D^{\mu}$ controller to a nonlinear two-mass system [7]. Wang and Gao [8] designed a PD^{μ} controller, and Petras [9] came up with tuning, auto-tuning and self-tuning methods for the FOPID. By using particle swarm optimization (PSO), Ramezani et al. [10] presented a method to optimally tune the practical FOPID controller's parameters for an automatic voltage regulator system.

Compared with conventional IOPID (integer-order PID), FOPID has low sensitiveness to external disturbances, and it also possesses unique characteristics in infinite dimensions. Furthermore, by applying FOPID to the control system, it can obtain fine tracking accuracy, abundant dynamics, high robustness and the like. There are two typical fractional-order operations, i.e., I and D in a

✉ Xiaojun Zhou
michael.x.zhou@csu.edu.cn

¹ School of Information Science and Engineering, Central South University, Changsha 410083, China

controller of FOPID, and thus, two additional parameters: the integral and differential order, denoted by λ and μ , respectively, should be taken into account, while the proportional, derivative and integral gains K_p , K_i , K_d are set. When $\lambda = 1$ and $\mu = 1$, it will become IOPID.

For POPID, parameter optimization is required for the specification compliance of the users in a certain process to find a series of optimal K_p , K_i , K_d , λ and μ values, which makes the adjustment problem of FOPID controller more complicated than classical PID control due to two additional arguments. Up to present, multifarious parameter setting methods have been proposed. In frequency domain, an evolutionary optimization scheme (EOS) to optimally determine the parameters of FOPID was proposed from loop-shaping perspective in [11]. For the FOPID controller design, an applied case of differential evolution was described by Arijit, which includes fractional-order integrator as well as fractional-order differentiator [12]. In time domain, [13] showed that the allowable parameters of PID controller can be determined by a small gain type, which is used previously in finite dimensional plants. Lee and Chang [14] came up with an evolutionary algorithm based on the electromagnetism-like algorithm, which is named IEMGA, to solve the problem of $PI^\lambda D^\mu$ controller parameters tuning. Padhee et al. [15] proposed a novel tuning method for tuning λ and μ of FOPID using genetic algorithms.

Recently, a novel stochastic method, i.e., the state transition algorithm (STA), has emerged in global optimization, where a solution to an optimization problem can be treated as a state, and in the meanwhile, the update of current solution using state transformation operators is considered as a state transition [16–19]. Using the state space representation, the state transition algorithm can describe solutions updating in a unified framework, and the execution operators to update solutions are expressed as state transition matrices, which make it easy to understand and flexible to implement. The strong global search ability and adaptability of state transition algorithm have been demonstrated by comparison with other global optimization algorithms and several real-world applications. Zhou et al. [20] applied the discrete state transition algorithm to solve the optimal design problem arising in water distribution networks. And in the meanwhile, Wang [21] used a multiobjective state transition algorithm in the alumina evaporation process to solve the problem of how to maintain the balance of operating costs and energy efficiency. In [22], in the case of small signals overlapping, a continuous STA was used to resolve the overlapping linear sweep voltammetric peaks to a very big one. Due to its powerful potential for finding a global minimum, in this study, we use STA to tune FOPID controller parameters via optimization.

In the meanwhile, it is found that both the objective criterion and the sample size have important impact on the performance of FOPID controller design, which can be easily neglected by most researchers. As a result, the influence of objective criterion and sample size on the performance of FOPID controller design is analyzed using simulation studies in this paper.

In what follows, the novelty and the contribution of this study are summarized: (i) A novel metaheuristic method called continuous state transition algorithm (STA) is introduced to solve the optimal design of $PI^\lambda D^\mu$ controller problem. Comparisons with STA with other optimization algorithms have testified that STA is a promising alternative method for FOPID controller parameters selection. (2) Different objective criteria and sample sizes are studied on the performance of FOPID controller design. (3) It is found that the integral time absolute error (ITAE) has the excellent tracking performance compared to other objective criteria.

The remainder of the study is organized as follows. Section 2 introduces the basics of fractional calculus and FOPID. Section 3 presents optimization problem formulation involving FOPID controller design. The state transition algorithm is then introduced in Sect. 4. In Sect. 5, some simulation results are given to illustrate the effectiveness of the proposed approach. The main conclusions of this paper are drawn in Sect. 6.

2 Fractional-order PID (FOPID) controller

FOPID controller is a generalization of conventional integer-order PID controller. Before the detailed form of FOPID controller, some fundamentals of fractional calculus are briefly introduced.

2.1 Fractional calculus

Fractional calculus, denoted as ${}_t \mathcal{D}_t^\kappa$ (where κ represents the fractional order, and t_0 and t represent the lower and upper limits of the operation, respectively), is a generalization of integration and differentiation to noninteger-order operator, which can be expressed as

$${}_t \mathcal{D}_t^\kappa = \begin{cases} \frac{d^\kappa}{dt^\kappa} & \kappa > 0, \\ 1 & \kappa = 0, \\ \int_{t_0}^t (dt)^{-\kappa} & \kappa < 0, \end{cases} \quad (1)$$

where $\kappa \in \mathbb{R}$ is generally assumed to be a real number.

There are several definitions to describe the fractional calculus, of which Riemann–Liouville and Grunwald–Letnikov definitions are most commonly used.

1. Riemann–Liouville definition (RL)

$${}_0\mathcal{D}_t^\kappa f(t) = \frac{1}{\Gamma(n-\kappa)} \frac{d^n}{dt^n} \int_{t_0}^t \frac{f(\tau)}{(t-\tau)^{1-(n-\kappa)}} d\tau$$

$$n-1 < \kappa < n$$

where $\Gamma(\cdot)$ is the Euler’s gamma function defined by

$$\Gamma(z) = \int_0^\infty t^{z-1} e^{-t} dt, \quad \mathbf{R}(z) > 0. \tag{3}$$

2. Grunwald–Letnikov definition (GL)

$${}_0\mathcal{D}_t^\kappa f(t) = \lim_{h \rightarrow 0} \frac{1}{h^\kappa} \sum_{i=0}^{[(t-t_0)/h]} (-1)^i \binom{\kappa}{i} f(t-ih), \tag{4}$$

where $(-1)^i \binom{\kappa}{i}$ is the binomial coefficient of $(1-z)^\kappa$. A numerical computation method for calculating the fractional calculus can be described as follows

$${}_0\mathcal{D}_t^\kappa f(t) = \frac{1}{h^\kappa} \sum_{i=0}^{[(t-t_0)/h]} w_i^{(\kappa)} f(t-ih), \tag{5}$$

here,

$$w_0^{(\kappa)} = 1, \quad w_i^{(\kappa)} = \left(1 - \frac{\kappa+1}{i}\right) w_{i-1}^{(\kappa)}, \quad i = 1, 2, \dots \tag{6}$$

The Laplace transformation of fractional derivative and integral of $f(t)$ can be defined by

$$\mathcal{L}\{\mathcal{D}^{-\kappa} f(t)\} = s^{-\kappa} F(s),$$

$$\mathcal{L}\{\mathcal{D}^\kappa f(t)\} = s^\kappa F(s) - \sum_{i=0}^{n-1} s^i [\mathcal{D}^{\kappa-i-1} f(t)]_{t=0}, \tag{7}$$

$$n-1 < \kappa < n.$$

The RL definition is equivalent to the GL definition since $\binom{\kappa}{i} = \frac{\Gamma(\kappa+1)}{i! \Gamma(\kappa-i+1)}$, while the GL definition is more suitable for numerical calculation, and it is adopted in this study.

2.2 The form of FOPID controller

The transfer function of $PI^\lambda D^\mu$ controller, which was proposed by Podlubny [5] for the first time, has the form

$$G_c(s) = \frac{U(s)}{E(s)} = K_p + K_i s^{-\lambda} + K_d s^\mu \tag{8}$$

where K_p, K_i and K_d represent the proportional, integral and differential gains, respectively; λ and μ are integral and differential orders correspondingly.

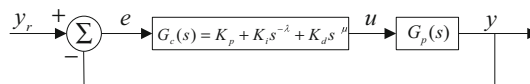


Fig. 1 Block diagram representation of system with $PI^\lambda D^\mu$ controller

When $\lambda = 1, \mu = 1$, there will be a special case of $PI^\lambda D^\mu$ controller:

$$G_c(s) = K_p + \frac{K_i}{s} + K_d s$$

It is not difficult to find that the above controller is a conventional integer-order PID controller. With the two extra parameters to be adjusted, the fractional-order PID controller is more flexible in controller design.

3 Optimization problem formulation

Figure 1 represents the block diagram with fractional-order controller. It is not difficult to obtain the closed-loop transfer function as follows

$$\frac{Y(s)}{Y_r(s)} = \frac{G_c(s)G_p(s)}{1 + G_c(s)G_p(s)} \tag{9}$$

where the $Y_r(s)$ and $Y(s)$ represent the control input and control output, respectively, $G_c(s) = \frac{U(s)}{E(s)} = K_p + K_i s^{-\lambda} + K_d s^\mu$ is controller of the system, and $G_p(s)$ is the transfer function of controlled plant.

From (9), the steady-state error of the closed-loop system is

$$E(s) = Y(s) - Y_r(s)$$

$$= \frac{G_p(s)G_c(s)}{1 + G_p(s)G_c(s)} Y_r(s) - Y_r(s) \tag{10}$$

where there are five unknowns, K_p, K_i, K_d and λ, μ . And then the objective function is defined as follows:

$$\min J_n(K_p, K_i, K_d, \lambda, \mu) \tag{11}$$

where $n = 1, 2, 3, 4$ represents the objective function under four different criteria, respectively, which are given by:

$$\left\{ \begin{array}{l} J_1 = \int_0^\infty [e(t)]^2 dt \\ J_2 = \int_0^\infty t[e(t)]^2 dt \\ J_3 = \int_0^\infty |e(t)| dt \\ J_4 = \int_0^\infty t|e(t)| dt \end{array} \right. \tag{12}$$

where $e(t) = y_r(t) - y(t)$ is the steady-state error; $y_r(t)$ and $y(t)$ are the reference input and the output signal, respectively. Moreover, J_1, J_2, J_3 and J_4 represent the integral squared error (ISE), integral time squared error (ITSE), integral absolute error (IAE) and integral time absolute error (ITAE) criteria, respectively. This paper will make a comparative analysis of these four kinds of criteria.

The equations in (12) are discretized, and the results are given by (13).

$$\begin{cases} J_1(m) = \sum_{m=1}^M e^2(m) \\ J_2(m) = \sum_{m=1}^M m e^2(m) \\ J_3(m) = \sum_{m=1}^M |e(m)| \\ J_4(m) = \sum_{m=1}^M m |e(m)| \end{cases} \quad (13)$$

where M represents the sample size. Since the integral range of criterion is $[0, \infty]$ in continuous state, M should approach ∞ ideally. And in this paper, the influence of sample size on the system response performance will be discussed.

Optimization algorithm can be used to find the controller parameters. Recently, state transition algorithm (STA) has been emerging as a very powerful method for global optimization (see [16–18]). Hence, we adopt STA to solve the problem of PI^2D^μ controller parameters tuning. In the sequel, we will give a brief of state transition algorithm.

4 Continuous state transition algorithm

In recent few years, a novel stochastic global optimization method, named state transition algorithm (STA), has been proposed [16–19], which is inspired by the notions of state transition and state space representation of control theory. In such a STA method, a solution to an optimization problem can be treated as a state; meanwhile, the update of current solution using state transformation operators is treated as a state transition. Generally, in continuous state transition algorithm, the unified form of generation of solution can be shown as follows:

$$\begin{cases} \mathbf{x}_{k+1} = A_k \mathbf{x}_k + B_k \mathbf{u}_k \\ y_{k+1} = f(\mathbf{x}_{k+1}) \end{cases}, \quad (14)$$

where $\mathbf{x}_k \in \mathbb{R}^n$ is a state, which corresponds to an optimization problem’s solution; A_k and B_k are state transition matrices which has suitable dimensions; \mathbf{u}_k is a function of \mathbf{x}_k as well as historical states, and f is considered as the evaluation function.

Four special operators of state transformation are developed on the base of multifarious type references of space transformation.

1. Rotation transformation (RT)

$$\mathbf{x}_{k+1} = \mathbf{x}_k + \alpha \frac{1}{n \|\mathbf{x}_k\|_2} R_r \mathbf{x}_k, \quad (15)$$

where α is defined as rotation factor and is a positive constant; $R_r \in \mathbb{R}^{n \times n}$ is a random matrix of which elements are within $[-1, 1]$; $\|\cdot\|_2$ is the vector’s 2-norm.

2. Translation transformation (TT)

$$\mathbf{x}_{k+1} = \mathbf{x}_k + \beta R_t \frac{\mathbf{x}_k - \mathbf{x}_{k-1}}{\|\mathbf{x}_k - \mathbf{x}_{k-1}\|_2}, \quad (16)$$

where β is defined as translation factor and is a positive constant; $R_t \in \mathbb{R}$ is a random variable of which elements are within $[0, 1]$.

3. Expansion transformation (ET)

$$\mathbf{x}_{k+1} = \mathbf{x}_k + \gamma R_e \mathbf{x}_k, \quad (17)$$

where γ is defined as expansion factor and is a positive constant; $R_e \in \mathbb{R}^{n \times n}$ is a random diagonal matrix of which elements obey the Gaussian distribution.

4. Axesion transformation (AT)

$$\mathbf{x}_{k+1} = \mathbf{x}_k + \delta R_a \mathbf{x}_k \quad (18)$$

where δ is defined as axesion factor and is a positive constant; $R_a \in \mathbb{R}^{n \times n}$ is a random diagonal matrix of which elements obey the Gaussian distribution, and meanwhile, there is only one random position having nonzero value.

Now we use the following pseudocode to sketch out the process of the continuous STA.

Algorithm 1 Pseudocode of the continuous STA

Input:

maxiter: the maximum number of iterations

SE: search enforcement

Best: the initial solution

Output:

*Best**: the optimal solution

```

1: repeat
2:   if  $\alpha < \alpha_{\min}$  then
3:      $\alpha \leftarrow \alpha_{\max}$ 
4:   end if
5:   Best  $\leftarrow$  expansion(funfcn,Best,SE, $\beta$ , $\gamma$ )
6:   Best  $\leftarrow$  rotation(funfcn,Best,SE, $\alpha$ , $\beta$ )
7:   Best  $\leftarrow$  axesion(funfcn,Best,SE, $\beta$ , $\delta$ )
8:    $\alpha \leftarrow \frac{\alpha}{fc}$ 
9: until the specified termination criterion is met
10: Best*  $\leftarrow$  Best

```

As for detailed explanations, Algorithm 2 illustrates the process of expansion function in Algorithm 1.

Algorithm 2 Pseudocode of the expansion transformation in Algorithm 1

```

Input:
oldBest: the best solution in the last transformation
Output:
Best*: the best solution
1: fBest ← feval(funfcn,oldBest)
2: State ← op_expand(Best,SE,γ)
3: [newBest,fGBest] ← fitness(funfcn,State)
4: fGBest ← feval(funfcn,newBest)
5: if fGBest < fBest then
6:   fBest ← fGBest
7:   Best ← newBest
8:   State ← op_translate(oldBest,Best,SE,β)
9:   [newBest,fGBest] ← fitness(funfcn,State)
10:  if fGBest < fBest then
11:    fBest ← fGBest
12:    Best ← newBest
13:  end if
14: end if
    
```

Where SE is search enforcement which represents the times of transformation by a certain operator, and a new best solution is adopted by using the “greedy criterion.” Besides, there are four other important parameters, namely rotation factor α , translation factor β , expansion factor γ and axesion factor δ . And *funfcn*, *Best* and *State* represent the objective function, the current best solution and the candidate solution set, respectively. And the specified termination criterion is the maximum number of iterations (Maxiter for short) in this study. In addition, in the case when a better solution can be found by other transformation operators except translation, the translation operator needs to be implemented.

In the continuous state transition algorithm, the rotation transformation can search in a hypersphere when a radius α is given coming from its ability of having the function of local search. The reduction of rotation factor α between a maximum value α_{max} and a minimum value α_{min} obeys an exponential way, of which the base *fc* is defined as lessening coefficient. The translation transformation is designed for a line search. The expansion transformation is developed for global search, of which the goal is searching with probability in whole space, and the axesion transformation is proposed in the late stage to strengthen the single-dimensional search as well as global search.

5 Simulation results

5.1 Simulation strategy

The test instances of the design problem are summarized in Table 1. The three problem instances which are taken

Table 1 Description of the problem instances considered

Problem number	Process plant transfer function G_p (s)
I	$\frac{5s^{0.6} + 2}{s^{3.3} + 3.1s^{2.6} + 2.89s^{1.9} + 2.5s^{1.4} + 1.7s^{1.2}}$
II	$\frac{1}{s^{3.5} + 10s^{2.8} + 35s^{2.1} + 50s^{1.4} + 24s^{0.7}}$
III	$\frac{s^{1.2} + 4s^{0.8} + 7}{8s^{3.2} + 9s^{2.8} + 9s^2 + 6s^{1.6} + 5s^{0.4} + 9}$

from [23] involve fractional-order plants, and in some cases, real systems can be better described by such transfer functions. All the examples of design obey the framework that is illustrated in Sect. 3. In the first place, we change the different objective criteria and sample sizes to study the influence of these two kinds of pre-conditions on the controller performance. Furthermore, we also run the other two state-of-the-art optimization algorithms, namely self-adaptive differential evolution (SaDE) algorithm [24] and comprehensive learning particle swarm optimization (CLPSO) algorithm [25], to compare with continuous STA.

For continuous STA, we use the same parameter settings as in previous [16], which are experimentally determined by carrying out a series of additional experiments with different parameters before conducting actual runs to obtain the results. The detailed parameters of continuous STA are given as follows: $\alpha_{max} = 1, \alpha_{min} = 1e-4, \beta = 1, \gamma = 1, \delta = 1, SE = 20, fc = 2, Maxiter = 20$.

Considering that the solution of (11) is a five-dimensional space which is $\{K_p, K_i, K_d, \lambda, \mu\}$. From the practical consideration of the $PI^{\lambda}D^{\mu}$ controller design, each parameter can be fixed within numerical ranges which are the same as them in [23]:

$$\begin{cases} 0 \leq K_p \leq 10 \\ 0 \leq K_i \leq 10 \\ 0 \leq K_d \leq 10 \\ 0 \leq \lambda \leq 2 \\ 0 \leq \mu \leq 2 \end{cases}$$

In what follows, 20 independent runs were carried out for each of the algorithms until the specified termination criterion is met, and in this paper it means the 20 iterations are met. Then we can observe the objective function value and the closed-loop system’s step response.

5.2 Study of objective criterion

In Sect. 3, four different criteria are given. First we choose the Problem I in Table 1 for simulation and then change the

Table 2 Steady-state error and controller parameters under different objective criteria

Problem number	Objective criterion	Minimum error	Controller transfer function G_c (s)
I	$\sum_{m=1}^M [e(m)]^2$	$5.104E-3$	$10 + \frac{1.324}{s^{0.01}} + 10s^{1.8011}$
	$\sum_{m=1}^M m[e(m)]^2$	$8.53E-4$	$9.5542 + \frac{1.434}{s^{0.5629}} + 10s^{1.4235}$
	$\sum_{m=1}^M e(m) $	$1.029E-3$	$4.0950 + \frac{3.6974}{s^{0.01}} + 5.5584s^{1.3698}$
	$\sum_{m=1}^M t e(m) $	$1.01E-4$	$10 + \frac{10}{s^{0.0617}} + 10s^{1.425}$

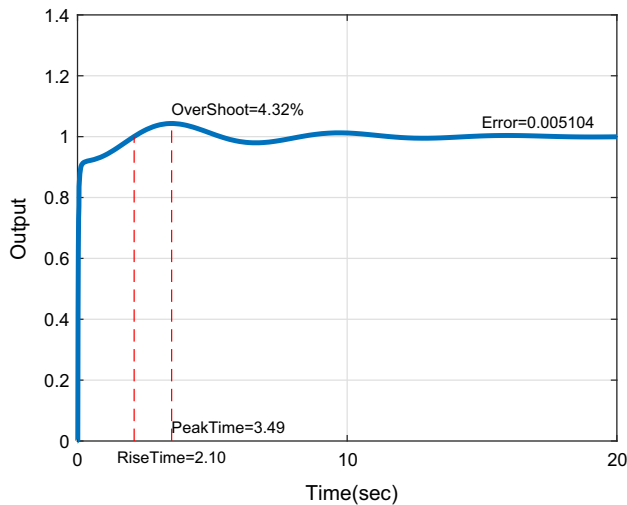


Fig. 2 Unit step response of closed-loop system for the Problem I with ISE

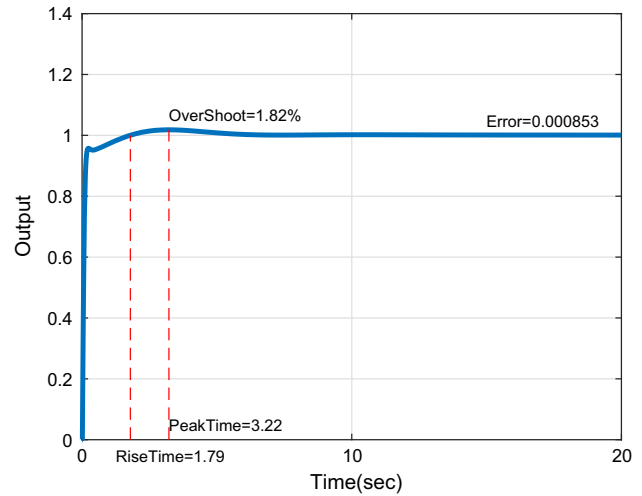


Fig. 3 Unit step response of closed-loop system for the Problem I with ITSE

different criteria. STA is applied to seek the optimal controller parameters.

The simulation results are given in Table 2 and Figs. 2, 3, 4 and 5. Table 2 reports the minimum steady-state error and controller parameters under different objective criteria. Figures 2, 3, 4 and 5 show the system response performance including the overshoot, rise time, peak time and the minimum steady-state error (the concepts are detailed in [26]). The graphs indicate that the ISE criterion can easily give rise to oscillation and cause the longest settling time for its performance index weights all errors equally independent of time. Moreover, its minimum steady-state error is $2.32E-3$, which is the biggest among the values obtained by all criteria. The ITSE criterion and IAE criterion can obtain bad steady-state error, and they need long settling time to stabilize the system. Besides, their other system response performance like rise time and peak time is bad. The ITAE criterion has excellent tracking performance, strong robustness and antidisturbance capability. Considering all kinds of factors, this paper decides to use the ITAE criterion to carry out the next experiment.

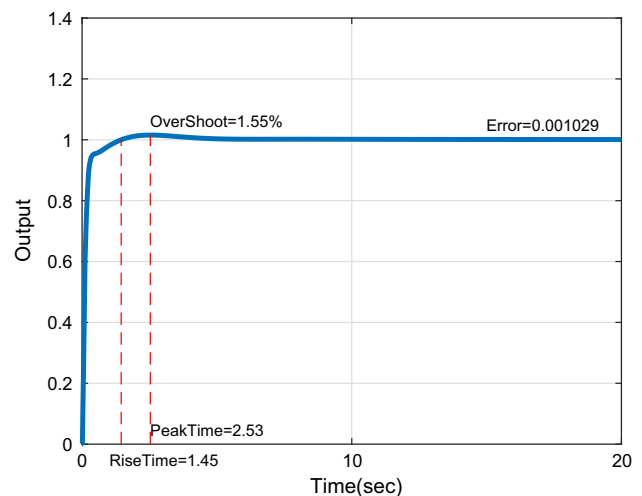


Fig. 4 Unit step response of closed-loop system for the Problem I with IAE

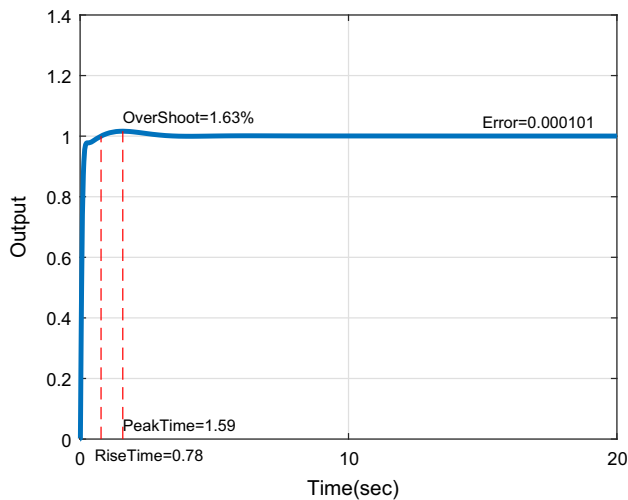


Fig. 5 Unit step response of closed-loop system for the Problem I with ITAE

5.3 Study of sample size

From (12) and (13) in Sect. 3, we have known the sample size M should approach to ∞ ideally. However, the sample size cannot be taken to infinity in real industrial process. In order to find a suitable sample size, simulation is carried

Table 3 Steady-state error and controller parameters under different sample sizes

Problem number	Sample size	Minimum error	Controller transfer function G_c (s)
I	1000	$2.034E-3$	$1.1498 + \frac{2.3940}{s^{0.2593}} + 8.6595s^{0.9591}$
	2000	$3.16E-4$	$10 + \frac{10}{s^{0.001}} + 10s^{1.245}$
	5000	$9E-6$	$10 + \frac{10}{s^{0.8462}} + 7.5432s^{0.9686}$

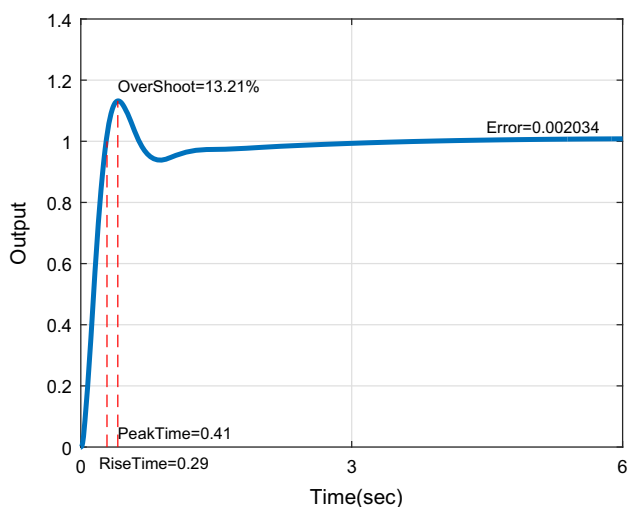


Fig. 6 Unit step response of system for the Problem I with sample size 1000

out under the different sample sizes as well as the same process plant (Problem I in Table 1) and objective criterion (ITAE).

The steady-state error is given in Table 3, and the unit step response is shown in Figs. 6, 7 and 8 based on different sample sizes. It is shown that the larger the sample size is, the smaller the steady-state error of the system step response will be. However, if the sample size increases, the parameters optimization time will increase. Besides, the response overshoots under sample size 1000 and sample size 5000 are 13.21 and 27.94 %, respectively, which are larger than the response overshoot under sample size 2000. Taking into account the practical efficiency and the response performance, this paper uses the sample size 2000.

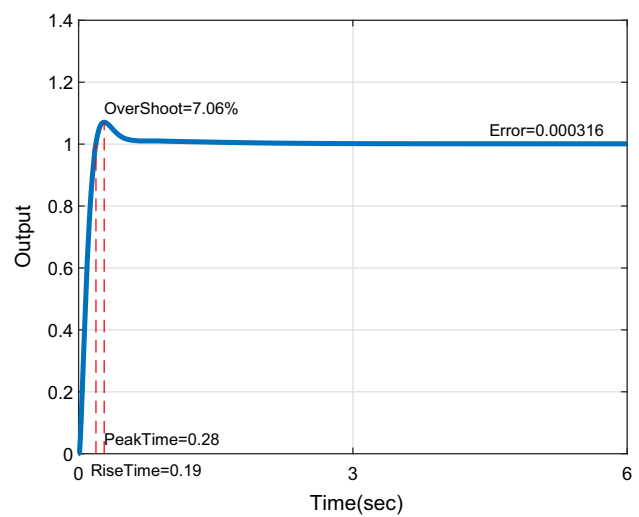


Fig. 7 Unit step response of system for the Problem I with sample size 2000

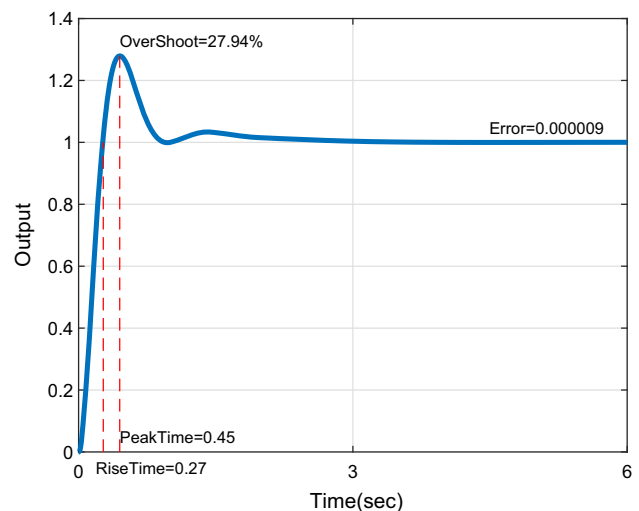


Fig. 8 Unit step response of system for the Problem I with sample size 5000

Table 4 Objective function values and controller parameters under different algorithms

Problem number	Methods	Best value	Mean value	SD	Worst value	Controller transfer function G_c (s)
I	STA	0.1285	0.1285	0	0.1285	$10 + \frac{10}{s^{0.01}} + 10s^{1.245}$
	SaDE	0.1452	0.1567	0.021	0.1666	$9.5542 + \frac{8.9385}{s^{0.0474}} + 5.5584s^{1.2446}$
	CLPSO	0.1352	0.1387	0.017	0.1447	$7.3583 + \frac{6.8519}{s^{0.2852}} + 6.0398s^{1.1973}$
II	STA	4.6079	4.6465	0.0226	4.6459	$10 + \frac{7.2089}{s^{0.3455}} + 10s^{0.4387}$
	SaDE	5.0012	5.2664	0.2414	5.5767	$8.3474 + \frac{4.7820}{s^{0.4294}} + 8.6702s^{0.6159}$
	CLPSO	4.7834	5.1128	0.33	5.5655	$8.2467 + \frac{4.6740}{s^{0.3475}} + 8.2459s^{0.7792}$
III	STA	0.1948	0.2199	0.0224	0.2491	$9.9453 + \frac{6.1539}{s^{1.3373}} + 5.434s^{1.1705}$
	SaDE	0.2655	0.3114	0.0439	0.3769	$9.445 + \frac{9.1731}{s^{1.3712}} + 5.4492s^{1.0898}$
	CLPSO	0.2542	0.3507	0.0997	0.4716	$7.6878 + \frac{6.5004}{s^{1.35}} + 5.466s^{1.1511}$

5.4 Comparison between STA and other algorithms

From the above observation, we find out the most suitable objective criterion and sample size. And then we will test STA on three instances in Table 1. Furthermore, the other two optimization algorithms are used for comparison.

Table 4 shows the results of $PI^{\lambda}D^{\mu}$ controller parameters and the objective function values for three test problems as found with optimization algorithms. All entries in this table are from the 20 independent runs of STA, SaDE, CLPSO algorithm. It should be noted that STA can obtain the best objective function value. And meanwhile the standard deviation can prove the stability of STA outperforms the other two algorithms. Figures 9, 10 and 11 report

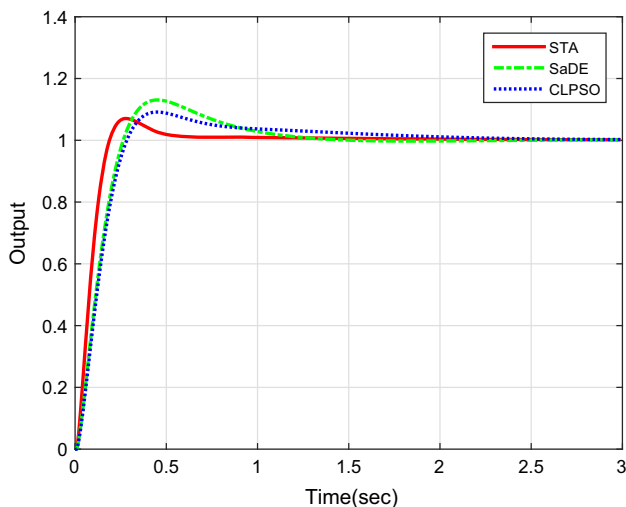


Fig. 9 Unit step response of the closed-loop system for the Problem I

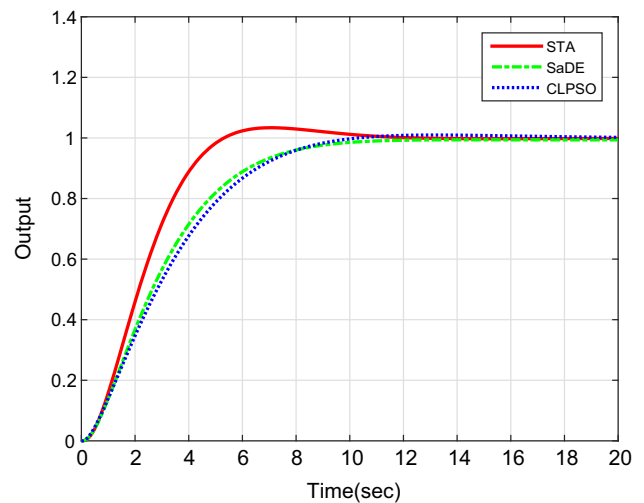


Fig. 10 Unit step response of the closed-loop system for the Problem II

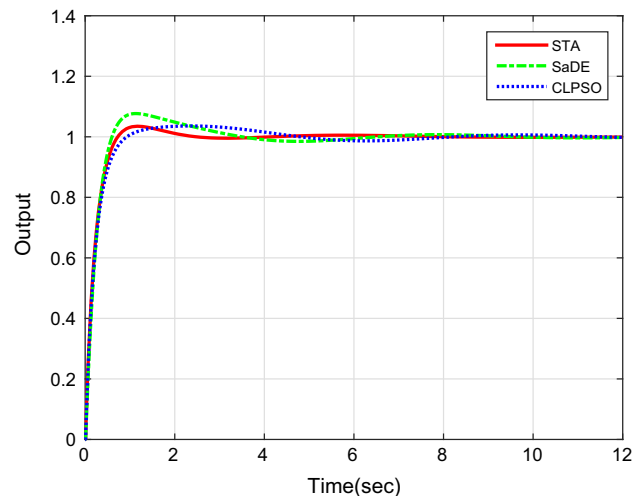


Fig. 11 Unit step response of the closed-loop system for the Problem III

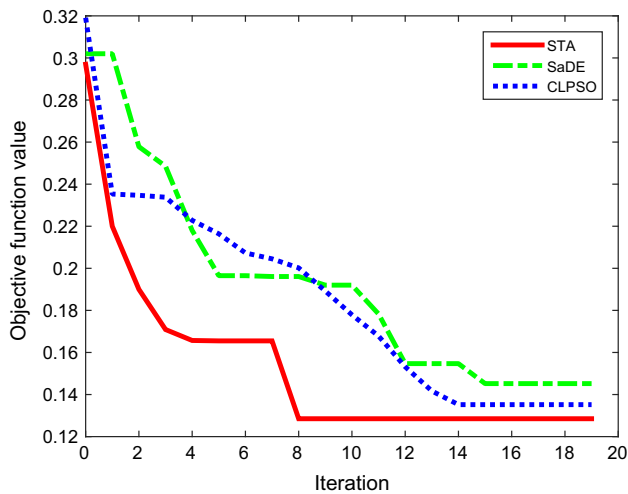


Fig. 12 Iterative curves of the objective function values obtained by different methods for Problem I

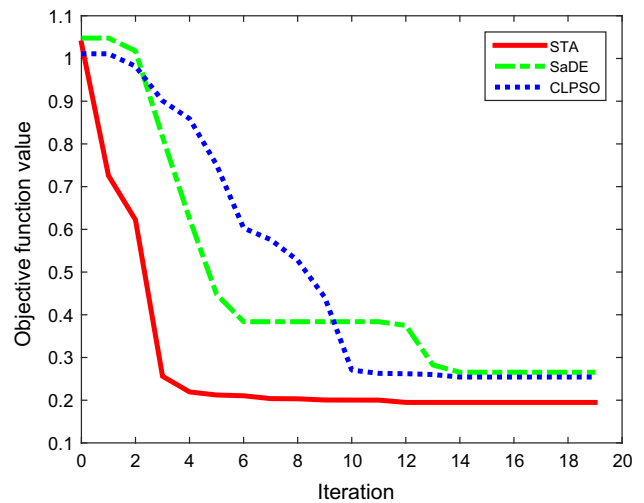


Fig. 14 Iterative curves of the objective function values obtained by different methods for Problem III

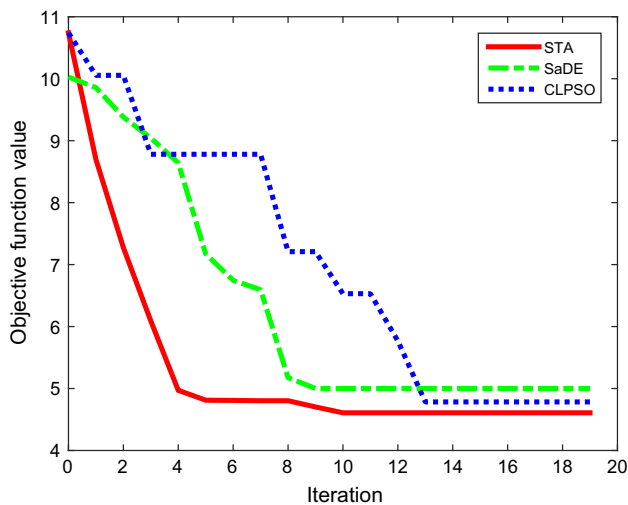


Fig. 13 Iterative curves of the objective function values obtained by different methods for Problem II

the dynamic response characteristics of the closed-loop systems as described in Table 1. The response performance involving overshoot, steady-state error, peak time and rise time demonstrates the superiority of STA. Furthermore, Figs. 12, 13 and 14 show the iterative curves of the objective function values obtained by different methods for the test problems, and it is obvious that STA could find much better solutions.

6 Conclusion

By taking the derivative order as well as integral order into consideration, designing FOPID controller will be more difficult than that of IOPID controller. The FOPID controller design problem can be converted into a parameter optimization problem, and it is found that the objective criterion and the sample size will affect the controller performance. In order to find the optimal FOPID controller parameters, we find the most suitable objective criterion and sample size by experiment at first. Then an intelligent optimization method, named state transition algorithm, is used to select these five optimal controller parameters. From the simulation results, it can be observed that the STA can be considered as an effective alternative method for FOPID controllers design.

Acknowledgments Authors thank the National Natural Science Foundation of China (Grant Nos. 61503416, 61533020, 61533021, 61590921) and Key Exploration Project (Grant No. 7131253) for the funding support.

Compliance with ethical standards

Conflict of interest We declare that there is no conflict of interest.

References

- Rai P, Shekher V, Prakash O (2012) Determination of stabilizing parameter of fractional order PID controller using genetic algorithm. *Int J Comput Eng Manag* 15:24

2. Sabatier J, Agrawal O, Machado J (2007) *Advances in fractional calculus*. Springer, Netherlands
3. Dadras S, Momeni H (2012) Fractional terminal sliding mode control design for a class of dynamical systems with uncertainty. *Commun Nonlinear Sci Numer Simul* 17(1):367–377
4. Krishna B (2011) Studies on fractional order differentiators and integrators: a survey. *Sig Process* 91(3):386–426
5. Podlubny I (1999) Fractional-order systems and PID controllers. *IEEE Trans Autom Control* 44(1):208–214
6. Das S, Pan I, Das S, Gupta A (2012) A novel fractional order fuzzy PID controller and its optimal time domain tuning based on integral performance indices. *Eng Appl Artif Intell* 25(2):430–442
7. Koksals E (2013) Fractional-order and active disturbance rejection control of nonlinear two-mass drive system. *IEEE Trans Ind Electron* 60(2):3806–3813
8. Wang D, Gao X (2012) H_∞ design with fractional-order PD controllers. *Automatica* 48(5):974–977
9. Petráš I (2012) Tuning and implementation methods for fractional-order controllers. *Fract Calc Appl Anal* 15(2):282–303
10. Ramezani H, Balochian S, Zare A (2013) Design of optimal fractional-order PID controllers using particle swarm optimization algorithm for automatic voltage regulator (avr) system. *J Control Autom Electr Syst* 24(5):601–611
11. Gao Q, Chen J, Wang L, Xu S, Hou Y (2013) Multiobjective optimization design of a fractional order PID controller for a gun control system. *Sci World J* 2013(1):907256–907256
12. Biswas A, Das S, Abraham A, Dasgupta S (2009) Design of fractional-order PID controllers with an improved differential evolution. *Eng Appl Artif Intell* 22(2):343–350
13. Özbay H, Bonnet C, Fioravanti A (2012) PID controller design for fractional-order systems with time delays. *Syst Control Lett* 61(1):18–23
14. Lee C, Chang F (2010) Fractional-order PID controller optimization via improved electromagnetism-like algorithm. *Expert Syst Appl* 37(12):8871–8878
15. Padhee S, Gautam A, Singh Y, Kaur G (2011) A novel evolutionary tuning method for fractional order PID controller. *Int J Soft Comput Eng* 1(3):1–9
16. Zhou X, Yang C, Gui W (2012) State transition algorithm. *J Ind Manag Optim* 8(4):1039–1056
17. Zhou X, Gao DY, Yang C (2013) A comparative study of state transition algorithm with harmony search and artificial bee colony. *Adv Intell Syst Comput* 213:651–659
18. Zhou X, Yang C, Gui W (2014) Nonlinear system identification and control using state transition algorithm. *Appl Math Comput* 226:169–179
19. Zhou X, Gao DY, Yang C, Gui W (2016) Discrete state transition algorithm for unconstrained integer optimization problems. *Neurocomputing* 173:864–874
20. Zhou X, Gao DY, Simpson AR (2016) Optimal design of water distribution networks by a discrete state transition algorithm. *Eng Optim* 48(4):603–628
21. Wang Y, He H, Zhou X, Yang C, Xie Y (2016) Optimization of both operating costs and energy efficiency in the alumina evaporation process by a multi-objective state transition algorithm. *Can J Chem Eng* 94(1):53–65
22. Wang G, Yang C, Zhu H, Li Y, Peng X, Gui W (2016) State-transition-algorithm-based resolution for overlapping linear sweep voltammetric peaks with high signal ratio. *Chemometr Intell Lab Syst* 151:61–70
23. Monje C, Chen Y, Vinagre B, Xue D, Feliu-Batlle V (2010) *Fractional-order systems and controls: fundamentals and applications*. Springer, Berlin
24. Qin A, Huang V, Suganthan P (2009) Differential evolution algorithm with strategy adaptation for global numerical optimization. *IEEE Trans Evol Comput* 13(2):398–417
25. Liang J, Qin A, Suganthan P, Baskar S (2006) Comprehensive learning particle swarm optimizer for global optimization of multimodal functions. *IEEE Trans Evol Comput* 10(3):281–295
26. Barbosa RS, Machado JT, Ferreira IM (2004) Tuning of PID controllers based on bodes ideal transfer function. *Nonlinear Dyn* 38:305–321